International Symposium on Notch Fracture (ISNF)
Santander (Cantabria, Spain), March 29-31, 2017

ANALYSIS OF THE DAMAGE EVOLUTION IN STEEL SPECIMENS UNDER TENSION BY MEANS OF XRCT

F. Suárez[a]*, J.C. Gálvez[b], D.A. Cendón[c], J.M. Atienza[c], F. Sket[d], J. Molina-Aldareguia[d]

[a]Departamento de Ingeniería Mecánica y Minera. Universidad de Jaén. Campus Científico-Tecnológico de Linares. Avda. de la Universidad (Cinturón Sur) 23700-Linares (Jaén)
[b]Departamento de Ingeniería Civil- Construcción. Universidad Politécnica de Madrid . E.T.S.I. Caminos, Canales y Puertos, C/ Profesor Aranguren s/n 28040 – Madrid, Spain
[c]Departamento de Ciencia de Materiales, Universidad Politécnica de Madrid . E.T.S.I. Caminos, Canales y Puertos, C/ Profesor Aranguren s/n 28040 – Madrid, Spain
[d]Instituto IMDEA Materiales, C/ Eric Kandel 2, Tecnogetafe 28906 – Madrid, Spain

* Contact person: fsuarez@ujaen.es

ABSTRACT

When a steel specimen is tested under tension, damage usually develops evenly all along the specimen, finally necking and leading to the typical cup-cone fracture surface. Nevertheless, some steels present an unusual fracture pattern consisting on a plane fracture surface with a dark region in the centre of the fracture zone. In this contribution, the authors analyse the evolution of the internal damage by using X-ray computed tomography (XRCT) on 3mm-diametre specimens of two steels. The specimens are tested in subsequent loading steps, after each of which it is unloaded and analysed with XRCT. This procedure helps to identify the evolution of damage developed inside each specimen at predefined strain levels. XRCT reveals a very high initial porosity in the material with the cup-cone fracture pattern and a very low initial porosity in the other. In the latter, fracture is triggered by a concentrated internal damage that can be seen as an internal notch which produces a stress concentration that leads to the eventual failure.

KEYWORDS: Steel, XRCT, Damage Evolution.

1. INTRODUCTION

Steel is one of the most used building materials and has been studied for a very long time. Tensile test [1] is the most used experimental procedure to characterise this type of materials, but it only allows obtaining the behaviour before necking develops, which usually leads to neglect the material behaviour after necking. In fact, some fracture mechanisms involved that lead to engineering problems in real life still remain unclear.

It is commonly accepted that fracture in metals is the result of a process of nucleation, growth and coalescence of microvoids [2]. It is also usual to observe that cylindrical metallic specimens subjected to tensile loading tend to show a well-known cup-cone fracture surface [3, 4]; nevertheless, this is not always the case. For example, eutectoid steel bars that are used for manufacturing prestressing wires show a flat surface with a dark circular region around the centre of it. Both fracture patterns can be observed in Figure 1. Cup-cone fracture pattern has been deeply studied in the past and many numerical models have been developed, which successfully reproduce the experimental observations [4, 5, 6, 7].

In previous works [8, 9, 10], the authors analysed the second fracture pattern considering that fracture was triggered by an internal damage zone. According to this hypothesis, the circular dark region observed in the fracture surface corresponds to the damage zone generated by nucleation, growth and coalescence of microvoids, which increases as applied load becomes higher. Once the damage zone gets a certain size, fracture develops in a brittle manner. This was analysed with tools usually applied in Linear Elastic Fracture Mechanics, like a modified cohesive model [9] and the formula by Guinea, Rojo and Elices [10], which predicts the size of an internal circular notch that triggers fracture for a certain load. Both approaches gave reasonable results.

In this contribution, the authors study damage evolution in two cylindrical steel specimens under tensile testing, one of a material that presents the typical cup-cone fracture pattern and the other one the flat surface with

the dark region mentioned before. X-ray computed tomography (XRCT) allows detecting internal voids or fracture regions inside a material, which here helps to identify the internal damage evolution.

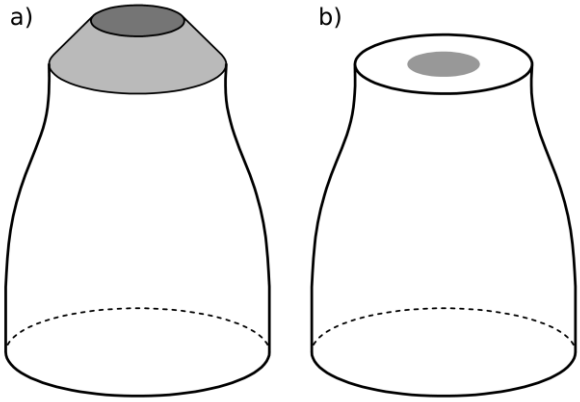

Figure 1. a) Cup-cone fracture pattern; b) Fracture pattern exhibited by eutectoid steel bars used for manufacturing prestressing wires.

2. EXPERIMENTAL WORK

2.1. Materials

a) Material 1

To produce steel wires used in prestressed concrete structures, raw eutectoid steel bars are cold-drawn, reducing their section and improving some mechanical properties of the material, making it more suitable for their final use [11, 12, 13]. Nevertheless, this process induces residual stresses in the steel bar so, to avoid the uncertainties derived from them, the specimen used in this study was obtained from a raw eutectoid steel bar before cold-drawing.

The chemical composition of this material can be consulted in Table 1.

Table 1. Chemical composition of Material 1

C (%)	Si (%)	Mn (%)	P (%)	S (%)	Cr (%)	Mo (%)
0.83	0.25	0.72	0.012	0.004	0.24	<0.01

Ni (%)	Cu (%)	Al (%)	Ti (%)	Nb (%)	V (%)	N (%)
0.02	0.01	<0.003	<0.005	<0.005	<0.01	0.0097

b) Material 2

This material corresponds to standard steel used as passive reinforcement in concrete structures. The steel used here is referred to as B 500 SD, according to the Spanish standard UNE 36068:2011 [14], with high ductility and an elastic limit f_t of 500N/mm^2.

Table 2 shows the chemical composition of this material.

Table 2. Chemical composition of Material 2

C (%)	Si (%)	Mn (%)	P (%)	S (%)	Cr (%)	Mo (%)
0.22	0.18	1.00	0.024	0.042	0.08	0.03

Ni (%)	Cu (%)	Al (%)	Ti (%)	Nb (%)	V (%)	N (%)
0.14	0.46	<0.003	<0.005	<0.005	<0.01	0.0113

2.2. Specimens

For both materials, 3mm-diameter specimens were tested; dimensions can be consulted in Figure 2.

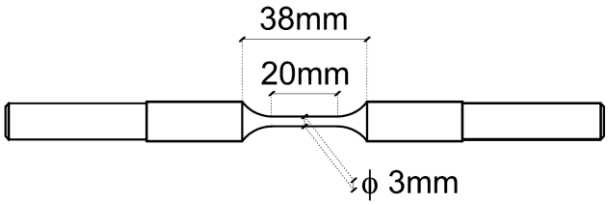

Figure 2. Specimens dimensions

The use of such a small diameter facilitates the penetration of X-rays in the specimens to identify internal damage.

2.3. Testing procedure

For both specimens, the same procedure was applied. Firstly, the specimen was analysed with the XRCT (Nanotom 160NF, Phoenix) before testing in order to obtain an initial picture of internal voids which would help comparing later images.

Then, the specimen was tested under tension up to the maximum load point in the load-strain curve (see Figures 3 and 5); once the maximum load was reached, the test was stopped and the specimen unloaded and analysed by XRCT. Afterwards, the specimen was tested under tension again up to a higher strain state, unloaded and anlysed by XRCT. This process was repeated for several strain states and until the specimen eventually failed.

Tables 3 and 4 show the predefined strain levels used in the described process for both materials. The strain values correspond to engineering strain measured for an initial length of 12.5mm centered in the necking zone.

Table 3. Strain levels applied with Material 1

Stage	1	2	3	4
ε_{eng}	0.076	0.104	0.118	0.124

Table 4. Strain levels applied with Material 2

Stage	1	2	3	4	5
ε_{eng}	0.193	0.267	0.288	0.306	0.319

The tomographic images were obtained at 80kV and 140mA using a tungsten target; the tensile tests were carried out with low speed displacement control and using a Suzpecar universal testing machine with a load cell of 100kN.

2.4. Results

Figures 3 and 4 show the load-strain curve of Material 1 with the analysed strain levels marked with blue points and the damage evolution observed by XRCT, where red areas correspond to low--density areas that can be identified as internal voids.

The same results for Material 2 can be observed in Figures 5 and 6.

3. DISCUSION

The initial tomographic image of both specimens, obtained before tensile testing, underlines the different nature of both materials. Material 1 presents almost no internal voids, whereas Material 2 has a high volume of them. It is also interesting to observe how these voids are lined up in the longitudinal direction of the specimen, probably due to the manufacturing process.

The different nature of both materials can also be observed in how differently both materials behave, not just in terms of stress, but also in terms of strain; while Material 1 reaches a maximum strain of about 0.13, Material 2 deforms up to around 0.34. This is also evident in the fact that Material 1 does not neck much, while necking is pretty noticeable in Material 2. Figure 7 shows the profiles of both specimens obtained by means of a Nikon V-12B profile projector.

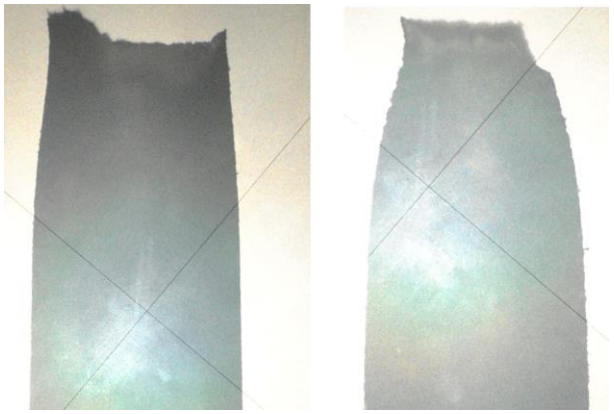

Figure 7. Specimens shapes after fracture; shape for Material 1 specimen on the left and shape for Material 2 specimen on the right.

In Material 1, under maximum loading, some small voids can be noticed. In further strain states new voids appear, some of them apparently in a random manner but some others interestingly aligned in the loading direction. The most remarkable observation in this material has to do with the last obtained picture, corresponding to stage 4, an instant very close to failure. Before this image, the voids have appeared somehow independently, not connecting to each other, but here internal cracks seem to have formed, especially a large one in the center of the necking region, generating a large plane crack.

This observation agrees well with the hypothesis posed by the authors in former works [8, 9, 10]. It suggests that fracture is initiated by an internal crack that, once it reaches a certain size, acts as an internal notch that triggers a brittle fracture process. This is interesting since it allows assuming some models and tools that belong to the Linear Elastic Fracture Mechanics field, which work reasonably well, as [9] and [10] proves, for a material that is clearly elastic-plastic.

Regarding Material 2, as mentioned before, a high number of voids are present in the beginning of the test, even before any load is applied. As load becomes higher, voids increase in number and in volume. In comparison with Material 1, it is interesting to notice that no void coalescence can be observed. It is not clear if this means that coalescence takes place just instants before failure happens or if the test could not be stopped close enough to the failure moment, so internal fracture surfaces could be observed. According to the results by Bluhm and Morrisey [15], it could be expected to see a fracture plane perpendicular to the loading direction, which would form the flat surface of the cup-cone fracture pattern, and some inclined fracture planes, related to the shear planes of the cup-cone shape.

4. CONCLUSIONS

In this paper, the authors have analysed two steels with distinct failure patterns, one of them corresponding to eutectoid steel used for manufacturing wires for prestressing (Material 1) and another one to standard steel used as reinforcement in concrete (Material 2). The study has been carried out on 3mm-diameter cylindrical specimens, which have been tested under tension in subsequent incremental strain steps up to failure. With the use of XRCT the internal damage evolution has been identified.

Material 1 specimen presents a plane fracture surface with a circular dark region in the center of the fracture area, whilst Material 2 specimen presents the classical cup-cone fracture pattern.

Material 1 has almost no initial voids and a slight internal porosity is developed through the tensile test.

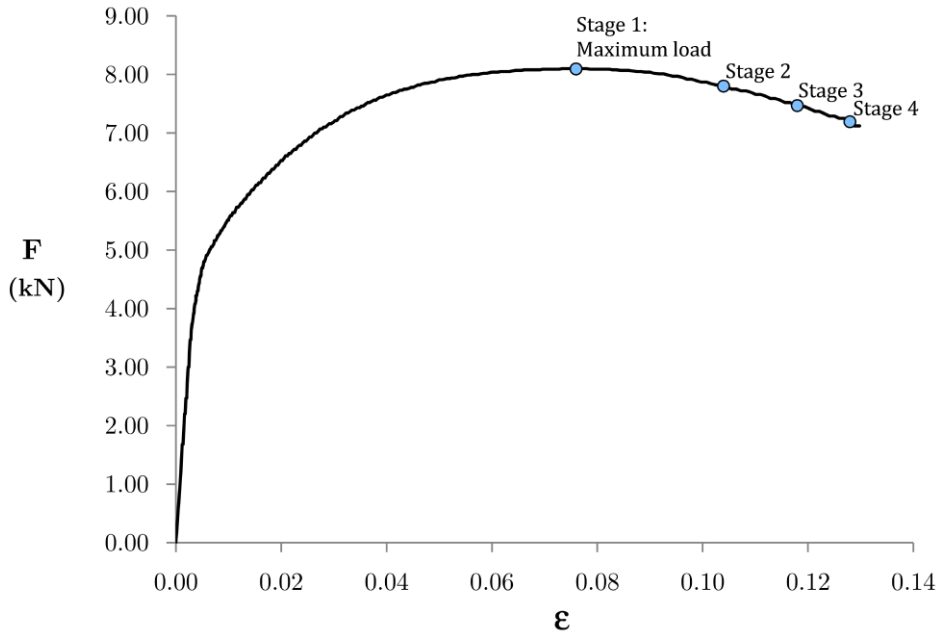

Figure 3. Load-strain curve of the specimen of Material 1. The load stages used to study the damage evolution are represented with blue circles.

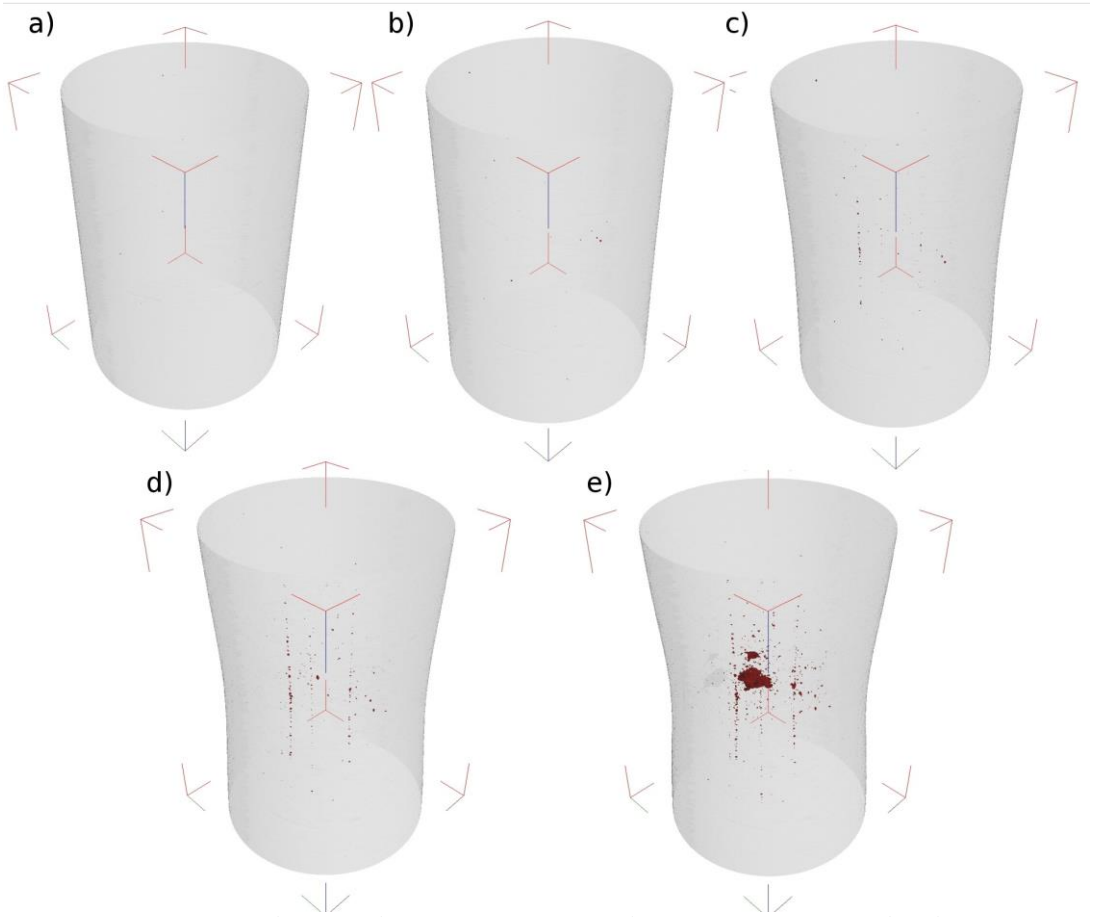

Figure 4. Damage evolution in the specimen of Material 1. Image a) correspond to the specimen before testing and images b)- f) to stages 1-4, respectively.

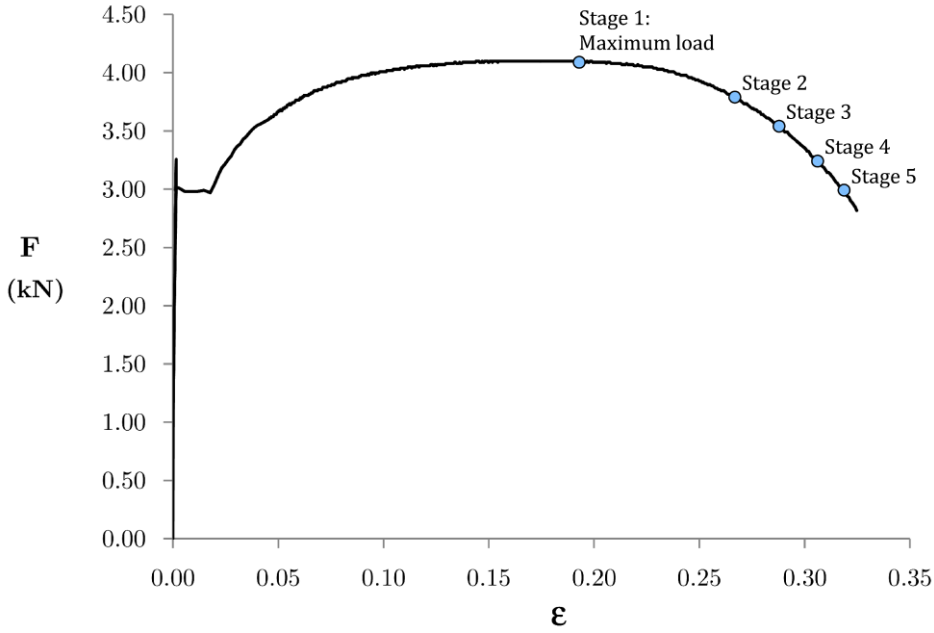

Figure 5. Load-strain curve of the specimen of Material 2. The load stages used to study the damage evolution are represented with blue circles.

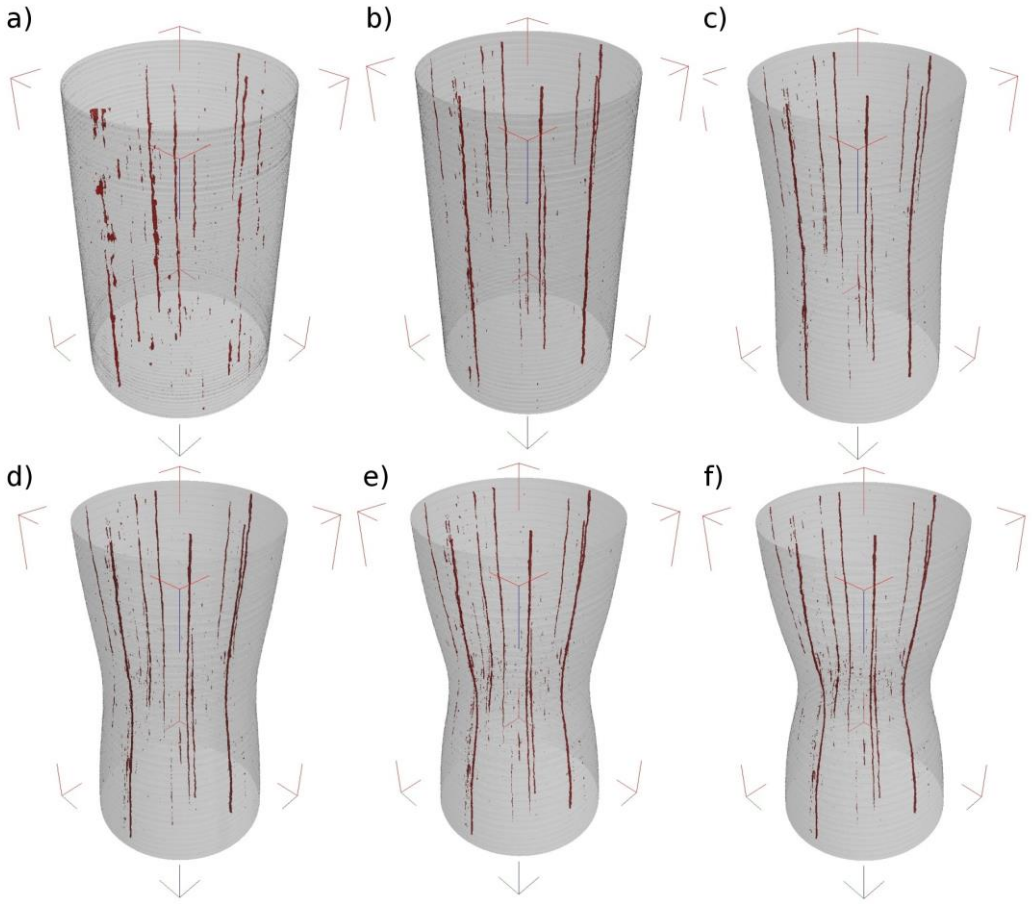

Figure 6. Damage evolution in the specimen of Material 2. Image a) correspond to the specimen before testing and images b)-f) to stages 1-5, respectively.

Just before failure, a large penny-shaped internal crack, perpendicular to the loading direction, is formed. This large internal crack acts as an internal notch which triggers fracture, which agrees well with previous works by the authors [9, 10].

Material 2 has a high initial porosity, probably due to the manufacturing process, which increases as the tensile test is carried out. In this case, no internal fracture planes have been observed, although, according to the observations by Bluhm and Morrisey [15], the progressive formation of the cup-cone fracture surface should be expected. This could be due to a very fast formation of this surface before fracture.

AKNOWLEDGEMENT

The authors want to express their gratitude to Luis del Pozo and Luisa Villares, from Emesa Trefilería, S.A. (Arteixo, La Coruña) for supplying the steel wires, as well as for providing their useful comments.

F. Suárez also wishes to express his gratitude to the Fundación Agustín de Betancourt for the grant provided.

REFERENCES

[1] ISO 6892-1:2009, Metallic materials. Tensile testing. Part 1: Method of test at room temperature.

[2] Anderson, T.L., Fracture Mechanics, fundamentals and applications, second edition. *CRC Press, Boca Raton*, 1995.

[3] Mirza, M.S., Barton, D.C., Church, P., Sturges, J.L., Ductile fracture of pure copper: an experimental and numerical study, *J. Phys. IV France* 7, C3, pp.891-896, 1997.

[4] Tvergaard, V., Needleman, A., Analysis of the cup-cone fracture in a round tensile bar, *Acta metall.* Vol. 32, No. 1, pp. 157-169, 1984.

[5] Johnson G.R., Cook W.H., A constitutive model and data for metals subjected to large strains, high strain rates and high temperatures, *Proceedings of the seventh international symposium on ballistics.* 1983.

[6] Gurson A.L., Porous rigid-plastic materials containing rigid inclusions: yield function, plastic potential and void nucleation. *International conference on fracture (ICF4), pp.357-364.* 1976.

[7] Gurson A.L., Continuum theory of ductile rupture by void nucleation and growth: Part I, yield criteria and flow rules for porous ductile media. *Part 1 in Technical report. Division of Engineering. Brown University*. 1977.

[8] F. Suárez, Estudio de la rotura en barras de acero. Aspectos experimentales y numéricos, Universidad Politécnica de Madrid, PhD Thesis, 2013.

[9] F. Suárez, J. C. Gálvez, D. A. Cendón, J. M. Atienza, Fracture of eutectoid steel bars under tensile loading: Experimental results and numerical simulation, *Engineering Fracture Mechanics*, Volume 158, 2016.

[10] F. Suárez, J. C. Gálvez, D. A. Cendón, J. M. Atienza, Study of the last part of the stress-deformation curve of construction steels with distinct fracture patterns, *Engineering Fracture Mechanics*, Volume 166, pp 43-59, 2016.

[11] J.M. Atienza, Tensiones residuales en alambres de acero trefilados, Universidad Politécnica de Madrid, PhD Thesis, 2001.

[12] Toribio, J., Ovejero, E., Effect of cumulative cold drawing on the pearlite interlamellar spacing in eutectoid steel, *Scr. Mater.* 39, pp. 323-328, 1998.

[13] González, B., Matos J.C., Toribio, J., Relación microestructura-propiedades mecánicas en acero perlítico progresivamente trefilado, *Anales de Mecánica de la Fractura* 26, Vol. 1, pp.142-147, 2009.

[14] UNE 36068:2011, Barras corrugadas de acero soldable para uso estructural en armaduras de hormigón armado.

[15] Bluhm, J.I., Morrisey, R.J., Fracture in a tensile specimen, *Proc. 1st Int. Conf. Fract.* 3, pp1739-1780, 1966.